Deep–Sea Research II 200 (2022) 105092

Contents lists available at ScienceDirect

Deep-Sea Research Part II

journal homepage: www.elsevier.com/locate/dsr2

Projected climate change impacts on the ecosystems of the Agulhas Bank, South Africa

Sarah Asdar [a,*], Zoe L. Jacobs [b], Ekaterina Popova [b], Margaux Noyon [a], Warwick H. Sauer [c], Michael J. Roberts [a,b]

[a] Nelson Mandela University, Ocean Sciences, Gqeberha, 6001, South Africa
[b] National Oceanography Centre, Southampton, SO14 3ZH, United Kingdom
[c] Department of Ichthyology and Fisheries Science, Rhodes University, Makhanda, South Africa

ARTICLE INFO

Keywords:
Agulhas bank
South Africa
Model
Future projections
Chokka squid
Climate change
Marine ecosystems

ABSTRACT

Marine ecosystems are expected to be increasingly affected by climate change, impacting their physical and biogeochemical environment. Changes in primary production, temperatures and hence species distribution, may lead to critical consequences for fishery exploitation. Therefore, future projections are essential to develop sustainable strategies and climate change adaptation plans for fisheries, and fishery-dependent societies. In this study, we focus on the Agulhas Bank, a broad extension of the continental shelf of the South African coast, along which flows the western boundary Agulhas Current. The Agulhas Bank is known for being biologically productive and is an important nursery ground for many commercially exploited fish species, including the chokka squid fishery, a vital source of income for many people in the Eastern Cape Province. Squid catches manifest strong interannual fluctuations, at times causing fishery crashes. Additional impacts due to climate change will have significant socio-economic consequences for this all-important fishery. To investigate future variations of the physical and biogeochemical environment on the Agulhas Bank, we used the global ocean model NEMO-MEDUSA, forced by the high emissions scenario RCP8.5. Our simulations show a significant increase in sea surface temperature and bottom temperature, but limited changes in primary production. Projections highlight an increase in current velocity on the Agulhas Bank throughout the course of this century, induced by an onshore shift of the Agulhas current. This current shift may pose a threat to squid recruitment success as a large fraction of squid paralarvae may be removed from their shelf feeding grounds and lost to the greater ocean via the Agulhas current. The results further show that planktonic food for the paralarvae is less likely to become the main limiting factor in the future, while increasing temperatures may affect growth rates and spawning success.

1. Introduction

The marine environment around southern Africa is diverse, complex and very variable (Lutjeharms et al., 2001) but also vulnerable to the impacts of climate change. Based on historical observations of sea surface temperature (SST), South Africa was identified as one of the 24 marine regions where observed warming was faster than the rest of the ocean and likely to continue in the future (Hobday and Pecl, 2014). Many of the marine hotspots are areas where human dependence on marine resources is very high. Thus, the impact of climate change on ocean dynamics could lead to potential changes in marine resource distribution or abundance and have a socio-economic impact on the population dependent on fisheries (Hobday and Pecl, 2014).

The productive waters of the coastal zone of South Africa provide an important source of food, jobs and livelihoods for tens of thousands of people living in the coastal areas (Cochrane et al., 2015). In the Eastern Cape, a province located in the southeastern part of South Africa and one of the most impoverished, the chokka squid (*Loligo vulgaris reynaudii*) fishery plays an important role in the economy of the region as a local employer (Roberts et al., in this issue). As the fourth most important fishery in South Africa, it employs around 3,000 people and is vital for around 25,000 people who are economically dependent on the performance of the fishery (Cochrane et al., 2014). The fishery is susceptible to periods of very low catches, which cause socio-economic strife in the region, for example in 1992 and 2001 (Ntola, 2010; Roberts, 2005). In 2013, the largest crash of the South African squid fishery was recorded

* Corresponding author.
E-mail address: sarah.asdar@gmail.com (S. Asdar).

https://doi.org/10.1016/j.dsr2.2022.105092
Received 6 July 2021; Received in revised form 31 March 2022; Accepted 9 April 2022
Available online 29 April 2022

and led to devastating consequences in the Eastern Cape (Joyner, 2015; Roberts et al., in this issue). The collapse is believed, by local fishermen, to be due to environmental changes as opposed to overfishing (Joyner, 2015).

Footprints of climate change have been reported for nearly all major marine ecosystems around the world (Hoegh-Guldberg and Bruno, 2010; Okey et al., 2014; Pecl et al., 2014; Wassmann et al., 2011), impacting their physical and biogeochemical environment. Such changes affect ecosystem processes and alter food webs (Brierley and Kingsford, 2009; Brown et al., 2010; Poloczanska et al., 2007), which consequently impact the distribution and abundance of species in some areas (Frusher et al., 2014; Mathis et al., 2015; Poloczanska et al., 2016).

Rouault et al. (2009) have shown that, since the 1980s, the SST of the Agulhas Current system has increased significantly. Moreover, based on satellite altimetry observations from 1993 to 2009, an intensification of the mesoscale activity of the Agulhas current has been highlighted (Backeberg et al., 2012) and it has been found that the current has broadened as a result of increased eddy activity (Beal and Elipot, 2016). Potts et al. (2015) suggest that changes in environmental conditions in the Agulhas Bank region will likely alter the migration of some species, affect the metabolism of the resident species and have negative implications in their recruitment. For example, an eastward shift in anchovy spawning distribution on the Agulhas Bank was suggested to be driven by a sudden change in SST in the region (Roy et al., 2007). This could have negative effects at higher trophic levels as it is an important prey for many fishes, birds and marine mammals (Cury et al., 2000).

Besides warming, acidification, deoxygenation and changes in primary productivity, considered as the key climatic stressors of ocean ecosystems induced by anthropogenic emissions of CO_2 (Bopp et al., 2013), more recent studies suggest that changes to ocean circulation in response to global warming is also a significant stressor (Popova et al., 2016; van Gennip et al., 2017; Jacobs et al., 2021). In this context, important changes have been observed in the strength and locations of some western boundary currents such as the East Australian Current, the Agulhas Current or the Kuroshio Current (Popova et al., 2016; Wu et al., 2012) with consequences for ecosystems beginning to emerge (Banks et al., 2010; Matear et al., 2013; Popova et al., 2016).

In this paper, we focus on the Eastern Agulhas Bank, the only area that provides optimal conditions to chokka squid for spawning (Roberts, 2005). This region is sustained by semi-permanent and intermittent coastal upwellings (Jacobs et al., in this issue), occurring between Port Alfred and Tsitsikamma (Downey et al., 2010) and is located east of a feature named the "Cold Ridge", commonly associated with high level of primary and secondary production (Boyd and Shillington, 1994). This feature is an upwelling filament resulting from an intense coastal upwelling along the Tsitsikamma coast combined with the westward-flowing mid-shelf current (Boyd and Shillington, 1994; Roberts, 2005; Jacobs et al., in this issue). It is considered an important nursery ground for squid paralarvae (Boyd and Shillington, 1994; Hancke, 2010). Roberts (2005) suggests that the westward current on the shelf transports the paralarvae towards this food source, known as the "Western Transport Hypothesis", which could mean that the variability of the local circulation patterns may have an impact on chokka squid recruitment (Hancke, 2010).

The aim of this study is to explore the projected changes on the wider Agulhas Bank region under the Representative Concentration Pathway 8.5 (RCP8.5) climate change scenario, in the high resolution coupled physical-biogeochemical model NEMO-MEDUSA. We focus our analysis on the climatic stressors of potential importance for the chokka squid population. The rest of the paper is organised as follows: the model simulation and observations used in this study are described in section 2, the performances of the model on the Agulhas Bank and the future projections are presented in section 3. The results are summarised and discussed in section 4.

2. Material and methods

2.1. Ocean model configuration

The coupled physical-biogeochemical model (hereafter, NEMO-MEDUSA) is a configuration developed in the Regional Ocean Acidification Modeling project (Yool et al., 2015). The projection analysed in this study was performed using version 3.5 of the Nucleus for European Modelling of the Ocean (NEMO) model. This is comprised of an ocean general circulation model, OPA (Madec, 2008), coupled with a sea-ice model, LIM2 (Timmermann et al., 2005). The horizontal resolution is approximately 1/4° and the model has 75 vertical levels increasing from 1 m thickness at the surface to 200 m at abyssal depths. Biogeochemistry in NEMO is represented by the plankton ecosystem model MEDUSA- 2 (Yool et al., 2013a; Yool et al., 2013b). This is a size-based, intermediate complexity model that divides the plankton community into "small" and "large" portions and which resolves the elemental cycles of nitrogen, silicon, and iron. The "small" portion of the ecosystem is intended to represent the microbial loop of picophytoplankton and microzooplankton, while the "large" portion covers microphytoplankton (specifically diatoms) and mesozooplankton (see Yool et al., 2013a for a full description of MEDUSA.). The model is forced at the surface by a simulation of the HadGEM2-ES Earth system model developed by the UK Meteorological Office (UKMO) which includes representations of the terrestrial and oceanic carbon cycles, atmospheric chemistry and aerosols (Collins et al., 2011). This simulation was performed as part of the UKMO's input to the Coupled Model Intercomparison Project 5 (CMIP5) (Jones et al., 2011) and Assessment Report 5 (AR5) of the Intergovernmental Panel on Climate Change (IPCC). The 1/4° simulation ran from start-1860 to end-2005 under historical atmospheric pCO_2 concentrations, and then from start-2006 to end-2099 under the IPCC RCP8.5 (Riahi et al., 2011). RCP8.5 is a scenario where CO_2 emissions increase over the 21st century, resulting in an additional radiative forcing of approximately 8.5 W m^{-2} by the end of the century. The physical part of the model is initialized using the same initial state as HadGEM2-ES and biogeochemistry is initialized from World Ocean Atlas (nutrients and oxygen) and GLODAP (dissolved inorganic carbon and alkalinity) climatology products. Due to its high computational cost, the model was initialized in 1975 from a 1° "twin" run from 1860 to 1975 under the same forcing dataset. Then, the model was integrated to end-2099. It does not allow any atmospheric feedback. Further details about model implementations can be found in Yool et al. (2013a, 2013b, 2015) and Popova et al. (2010).

2.2. AR5 comparison

Here, the biogeochemistry is analysed in a suite of CMIP5 models (Taylor et al., 2012) to assess where the NEMO-MEDUSA future projections belong in the multi-model ensemble for the southwest Indian Ocean, following (Jacobs et al., 2021). First, skill metrics are applied to compare observational data with the models in order to identify an "inner ensemble" of models that simulate the observations best. This inner ensemble is then used to frame the assessment of future projections from 2006 to 2100 under the RCP8.5 experiment. The selection of CMIP5 models used here (Table 1) is based on those that include the dissolved inorganic nitrogen (DIN) and Integrated primary production (PP).

Statistical metrics are employed to score the models on how well they reproduce the spatial pattern of DIN over the southwest Indian Ocean. DIN has been chosen because of good observational data coverage (here from the World Ocean Atlas, 2013; WOA13, Garcia et al., 2013) and because the key role played by macronutrients in framing marine productivity makes it a good indicator of the quality of a model's skills in respect to biogeochemistry. All models are linearly interpolated onto a standard 1° grid, to ensure consistency, and averaged over the first decade of the future projection run from 2006 to 2015. Over an

Table 1
List of CMIP5 models (and NEMO-MEDUSA) and their corresponding skill metric scores; the correlation coefficient, r, and the root mean square error, RMSE, when compared to climatological DIN from WOA13. Models in bold are not in the inner ensemble and are excluded from further analysis.

Modelling Centers	Model name	r	RMSE x10^{-3} [mmol.m^{-3}]
National Oceanographic Center Southampton	NEMO-MEDUSA	0.78	0.68
Canadian Centre for Climate Modelling and Analysis	CanESM2	0.61	0.76
Centro Euro-Mediterraneo sui Cambiamenti Climatici	CMCC-CESM	0.77	0.6
Centre National de Recherches Météorologiques/Centre Européen de Recherche et Formation avancée de Calcul Scientifique	CNRM-CM5	0.12	6.7
NOAA Geophysical Fluid Dynamics Laboratory	GFDL-ESM2G	0.67	0.53
	GFDL-ESM2M	0.77	0.41
NASA Goddard Institute for Space Studies	GISS-E2-H-CC	0.6	0.75
	GISS-E2-R-CC	0.64	0.59
Met Office Hadley Center	HadGEM2-CC	0.72	0.57
	HadGEM2-ES	0.71	0.58
Institut Pierre-Simon Laplace	IPSL-CM5A-LR	0.76	0.65
	IPSL-CM5A-MR	0.74	0.5
	IPSL-CM5B-LR	0.72	0.42
Japan Agency for Marine-Earth Science and Technology/Atmosphere and Ocean Research Institute (The University of Tokyo)/National Institute for Environmental Studies	MIROC-ESM	0.66	0.54
	MIROC-ESM-CHEM	0.66	0.55
Max-Planck-Institut für Meteorologie	MPI-ESM-LR	0.78	0.81
	MPI-ESM-MR	0.71	0.43
Meteorogical Research Institute	MRI-ESM1	0.69	0.43
Norwegian Climate Center	NorESM1-MR	0.61	1.1

extended region around southern Africa, most models represent the spatial distribution of DIN well, with realistic transition from greater concentrations in the Southern Ocean and in the Benguela upwelling system, to lower concentrations south of Madagascar (Supplementary Fig. 1). Despite this, there are some models that do not capture this large scale gradient while others underestimate DIN concentrations over the Agulhas Bank. To quantify this, skill metrics are calculated between the decadal mean of each model and WOA13 over the southwest Indian Ocean (38°S-25°S, 19-45°E). It is important to assess a region larger than the Agulhas Bank to ensure a realistic representation of the large-scale pattern by these relatively coarse resolution models. At the same time, the boundaries are restricted so that the metrics are not skewed by the steep gradient of nutrient concentrations in the Southern Ocean, which may skew the metrics towards models correctly reproducing this gradient, rather than relatively low background values of the subtropical Indian Ocean. The western boundary is also placed at 19°E to avoid the Benguela upwelling system, which is highly variable across the models and is outside the focus of this study. The metrics used are Pearson's correlation coefficient, *r*:

$$r = \frac{\sum_i (x_i - \bar{x})(y_i - \bar{y})}{\sqrt{\sum_i (x_i - \bar{x})^2}\sqrt{\sum_i (y_i - \bar{y})^2}}$$

where *x* and *y* are the observed and modelled data points respectively, and the root mean square error (*RMSE*):

$$RMSE = \sqrt{\sum_{i=1}^{n} \frac{(x_i - y_i)^2}{n}}$$

where *n* is the number of grid points. Combined, they capture the tendency of each model to vary with the observations and the magnitude of the discrepancies between them (Stow et al., 2009). The analysis here complements prior studies to provide model assessment for the tropical Indian Ocean (as in Allen et al., 2007; Stow et al., 2009; Bopp et al., 2013; Ilyina et al., 2013; Séférian et al., 2013; Cabré et al., 2015; Rickard and Behrens, 2016; Bao and Li, 2016; Mohan and Bhaskaran, 2020; Jacobs et al., 2021).

Table 1 lists the *r* and *RMSE* for each model. A large spread exists across both metrics with NEMO-MEDUSA and MPI-ESM-LR achieving the highest *r*, 0.78, and CNRM-CM5 the lowest, 0.12. CNRM-CM5 also has the largest RMSE, 6.7×10^{-3}, while GFDL-ESM2M has the lowest RMSE, 0.41×10^{-3}. Just one model, CNRM-CM5, falls outside the range of two standard deviations for each metric and is considered the "outer ensemble". The remaining models are characterised as the "inner ensemble" and are used to analyse the future projections of DIN and PP. The projected changes in DIN (averaged over the southwest Indian Ocean from 38°S-25°S, 19-45°E) are shown in Fig. 1. Besides CMCC-CESM projecting an increase of 429%, the rest of the models project an average decrease of 41% (ranging from 15 to 71%), with NEMO-MEDUSA projecting a reduction of 57%.

PP is shown as a decadal average over the first decade (2006–2015) of the future projection runs and from the observational product in Supplementary Fig. 2. Over the wider Agulhas Current region, the models generally simulate the spatial pattern of observed PP well, with elevated productivity in the Benguela upwelling system, while lower rates of production are found east of South Africa which is consistent with DIN availability. However, most models underestimate productivity over the Agulhas Bank, with observed values reaching 1.25 gC m^{-2} d^{-1}.

When calculating skill metrics, extra uncertainty is added when using observationally-estimated PP, which uses satellite-derived observations of chlorophyll and temperature together with productivity models rather than direct measurements (Anav et al., 2013). Thus, we use the same "inner ensemble" based on the skill metrics calculated for DIN. The projected changes in PP over the southwest Indian Ocean are shown in Fig. 2. Besides a projected increase of 56% by CMCC-CESM, consistent with a considerable DIN increase, and a smaller projected increase (3%) by GFDL-ESM2M, the inner ensemble models project a mean reduction of 18% (ranging from 1 to 38%) by 2100. With a decrease of 26% over the century, NEMO-MEDUSA is consistent with the "inner ensemble" projections.

For both variables, projected reductions in NEMO-MEDUSA are well within the range across all models. It also has higher baseline values for DIN and PP (2000–2010) that are actually closer to the observed mean, which could be due to its higher resolution leading to a more effective resolution of smaller-scale processes. HadGEM2-ES, used as the surface forcing for NEMO-MEDUSA, is one of the central ensembles and shows similar reductions to NEMO-MEDUSA (−38% and −58% for PP and DIN respectively). Overall, this analysis reveals that future projections of annual mean PP and DIN in NEMO-MEDUSA are consistent with CMIP5 models in the wider Agulhas Current region, which is consistent with the global ocean (Bopp et al., 2013; Kwiatkowski et al., 2020).

2.3. Observational datasets

In order to assess and validate the model, the following observational products are used. Decadal (2000–2009), annual (2005) and monthly (May 2005) means of modelled surface currents are compared to the Ssalto/Duacs altimeter product produced and distributed by the Copernicus Marine and Environment Monitoring Service (CMEMS). The zonal and meridional components of surface geostrophic velocities are derived from Absolute Dynamic Topography, which combine the Sea Level Anomalies with the CNES-CLS13 Mean Dynamic Topography (Rio et al., 2014). The data used in this study are derived from monthly

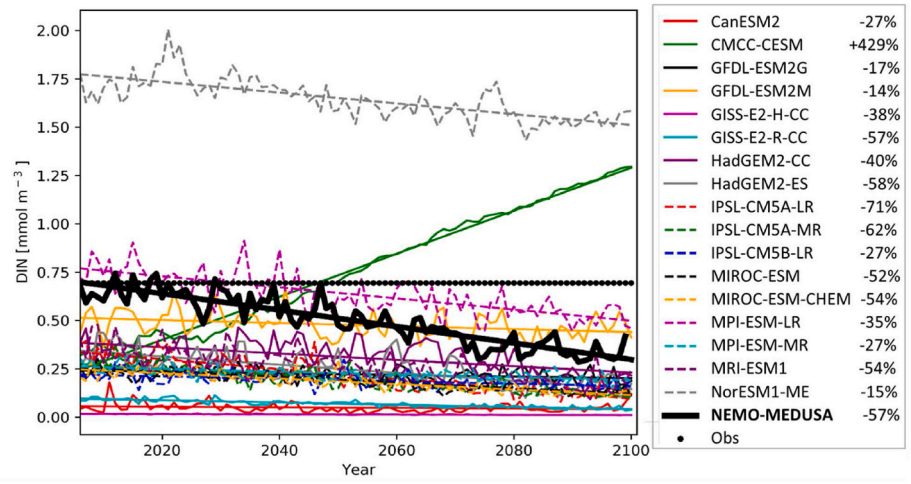

Fig. 1. Future projections of DIN (mmol m^{-3}) in the southwest Indian Ocean (38°S-25°S, 19°E−45°E) from 2006 to 2100 in the "inner ensemble" models, the WOA entry is the climatological mean from WOA13. The % change from 2006 to 2100 for each model is based on the overlaid trend lines.

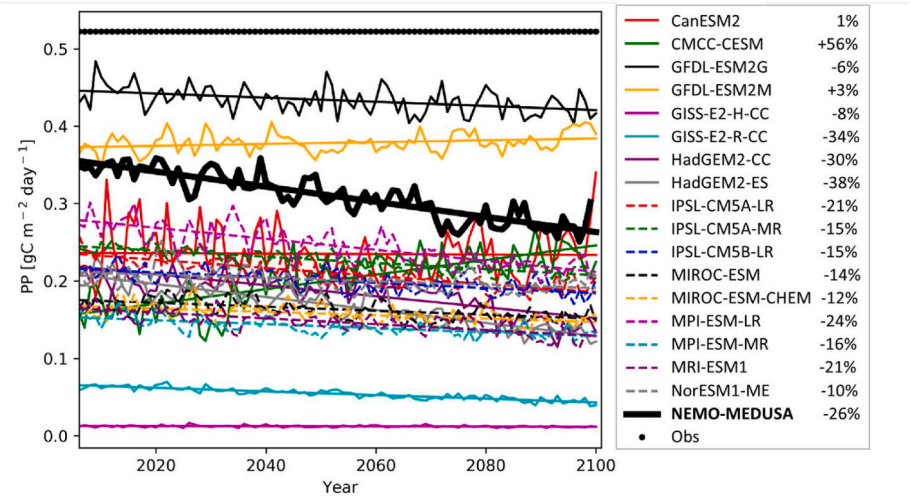

Fig. 2. Future projections of integrated PP (gC m^{-2} day^{-1}) in the southwest Indian Ocean (38°S-25°S, 19°E-45°E from 2006 to 2100 in the "inner ensemble" models, the "Obs" entry is the decadal mean from estimated observed integrated PP derived from satellites. The % change from 2006 to 2100 for each model is based on the overlaid trend lines.

averaged velocity fields (spatial resolution: 1/4°) and cover the period from January 2000 to December 2009.

The decadal-averaged (2000–2009) modelled SST fields are compared to the NOAA 1/4° daily Optimum Interpolation SST (OISST), version 2. The OISST product is an analysis constructed by combining observations from different platforms (satellites, ships, buoys) on a regular global grid (Banzon et al., 2016). A spatially complete SST map is produced by interpolating to fill in gaps. We use monthly data from 2000 to 2009.

The seasonal cycle of modelled depth-integrated PP is compared to the average of three datasets estimated by three empirical models: the VGPM (Behrenfeld and Falkowski, 1997), Eppley-VGPM (Carr et al., 2006) and CbPM (Westberry et al., 2008) productivity models. The seasonal cycle from monthly estimates from 2000 to 2009 is computed and used for this study.

The seasonal cycle of modelled DIN concentration is compared to in-situ nitrate concentrations from the World Ocean Database 2018 (WOD2018, Boyer et al., 2019), a product of NOAA's National Centers for Environmental Information (NCEI). The WOD is a collection of scientifically quality-controlled ocean profiles that include measurements of nitrate. Nitrate measurements are scarce and not homogeneous in space or time (Supplementary Fig. 3). Hence, observations are not restricted to the period 2000–2009 but all data available on the Agulhas Bank (from 1963 to 2019) is used.

The seasonal cycle of modelled Mixed Layer Depth (MLD), which is calculated as the first depth that the temperature is 0.1 °C different from the surface, is compared to that from the global annual climatology distributed by IFREMER/LOS (www.ifremer.fr/cerweb/deboyer/mld). This climatology is estimated from 5 million temperature profiles (measured from 1990 to 2008) using the method described in de Boyer Montégut et al. (2004). The global data is computed on a 2° resolution grid.

3. Results

3.1. Model validation on the Agulhas Bank

Before analysing the future projections, the model performance is validated over the wider Agulhas Current region and on the Agulhas Bank. Fig. 3 shows the surface currents as a decadal mean (2000–2009), an annual mean (2005) and a monthly mean (May 2005) in the model (right panels) and from satellite (left panels). Decadal-averaged values

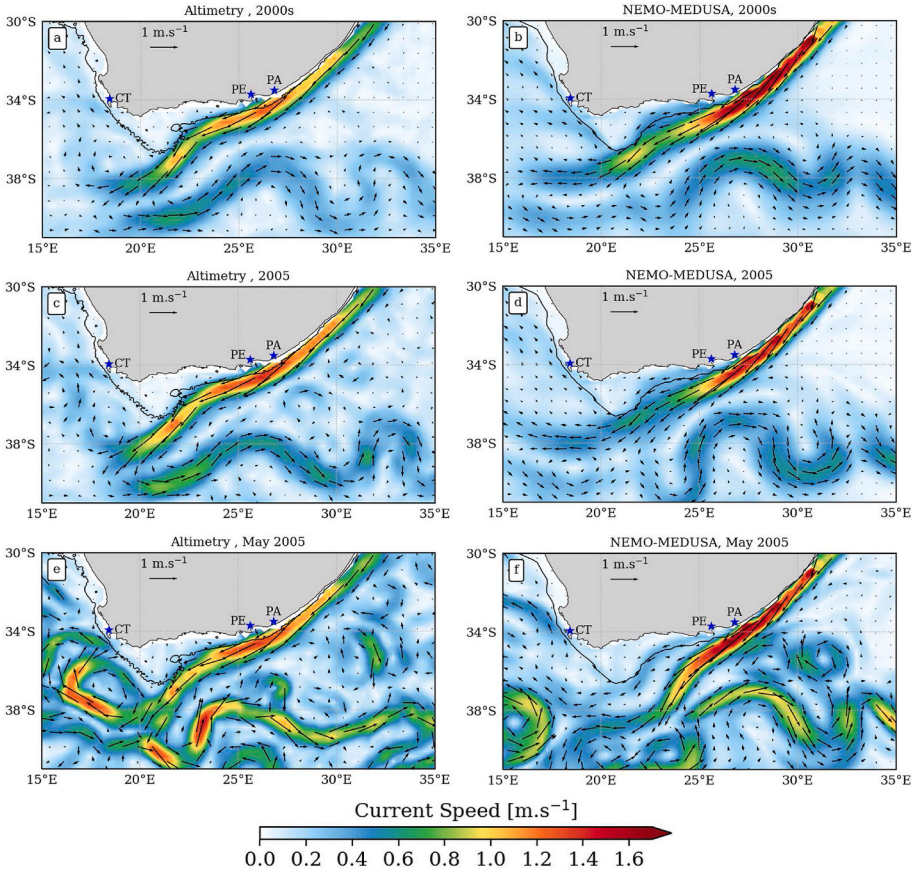

Fig. 3. Observational (left) and NEMO-MEDUSA (right) surface current velocity (m.s^{-1}) shown as a decadal mean, for 2000–2009 (a,b), an annual mean, 2005 (c,d) and a monthly mean, May 2005 (e,f). The colours represent the intensity of the current and the arrows its direction. Observational currents are derived from the satellite altimetry product from CMEMS. The 200 m isobath from ETOPO2 (left) and the model (right) is overlaid as a black line. CT, PE and PA stand for Cape Town, Port Elizabeth (now Gqeberha) and Port Alfred respectively.

highlight persistent features without being complicated by short-term variability (Fig. 3a and b). At this time scale, the model is able to simulate the Agulhas Current position well with flow running along the east coast of South Africa and along the Agulhas Bank, following the 200 m isobath, before being retroflected at 21°E to become the Agulhas Return Current. At an annual time scale (Fig. 3c and d), the model simulates the Agulhas Current accurately but with evidence of interannual variability in the position of mesoscale features which we do not expect the model to reproduce precisely, due to the stochastic component of the mesoscale variability (Jacobs et al., 2020; Robinson et al., 2016; Srokosz et al., 2015). At a monthly scale (Fig. 3e and f), it is able to simulate typical scales and topology of the mesoscale features and several Agulhas rings are also evident. However, at about 25°E there is a slight overshoot of the current for the three different time scales. There is also a second but weaker retroflection west of the main one occurring at 21°E. Correct placement of the Agulhas Current retroflection is known as one of the largest challenges in modelling the Agulhas Current and is better represented in a higher resolution model (see Jacobs et al., in this issue). However, it is unclear whether the correct positioning of this feature would impact the Agulhas Bank ecosystem.

East of 25°E, the strength of the Agulhas Current is represented well in the model, although velocities are slightly overestimated (with maximum values up to 1.7 m s^{-1}) compared with satellite altimetry data (up to 1.3 m s^{-1}). However, west of 25°E, the model tends to underestimate the Agulhas Current surface velocity.

Decadal-averaged (2000–2009) SST from the model and from observations are presented in Fig. 4. Fig. 4c, illustrating the difference between the two datasets, shows the largest anomaly in the Benguela upwelling and highlights an SST warmer in NEMO-MEDUSA than in the observations. In agreement with the observations (Fig. 4a), modelled SST fields (Fig. 4b) show the warmer surface waters of the Agulhas Current flowing along the Agulhas Bank with cooler water on the Agulhas Bank. Generally, observed and modelled values exhibit a similar distribution despite the fact that the model overestimates SST by up to 1 °C on the Agulhas Bank and in the Agulhas Current.

Fig. 5 shows the seasonal cycles of depth-integrated PP, surface DIN concentrations and MLD for the decade 2000–2009 from the model compared with observations. Seasonal cycles are computed on the Central Agulhas Bank (20°E−23°E, hereafter CAB), influenced by the cold ridge, and the Eastern Agulhas Bank (23°E−27°E, hereafter EAB) influenced by coastal upwellings and characterised by high concentrations of chlorophyll (Downey et al., 2010). These two areas of the Agulhas Bank are shown on Fig. 4.

PP estimates (Fig. 5a and b) are available for the same period as the model, whereas the MLD climatology has been computed from in-situ data measured over the period 1990–2008 (Fig. 5e and f). As nitrate data are scarce on the Agulhas Bank, we use all available data which span from 1953 to 2016 rather than a selection of points for the 2000–2009 period.

The satellite-derived PP displays a seasonal cycle more pronounced on the EAB than on the CAB, with values ranging from 0.73 to 1.36 gC.m^{-2}.d^{-1} on the CAB and from 1 to 2.05 gC.m^{-2}.d^{-1} on the EAB (Fig. 5a and b). A minimum, around July, and two maximums, March–April and October–November, are evident. A smaller seasonal range exists in the model across the whole Agulhas Bank, with a minimum from June–July and maximums in November and January. The modelled values range from 0.73 to 1.14 gC.m^{-2}.d^{-1} on the CAB and from 0.86 to 1.29 gC.m^{-2}.d^{-1} on the EAB. Even though the model struggles to catch the seasonal cycle on the EAB, likely due to shelf-edge and coastal dynamics not being parametrized well in NEMO-MEDUSA, the seasonal cycle on the CAB is fairly well represented. Note that satellite-derived PP is not represented by a direct observation but is an average of three estimates derived from remote sensing algorithms (VGPM, Eppley-VGPM and CbPM) hence it has to be taken with caution. Moreover, due to the

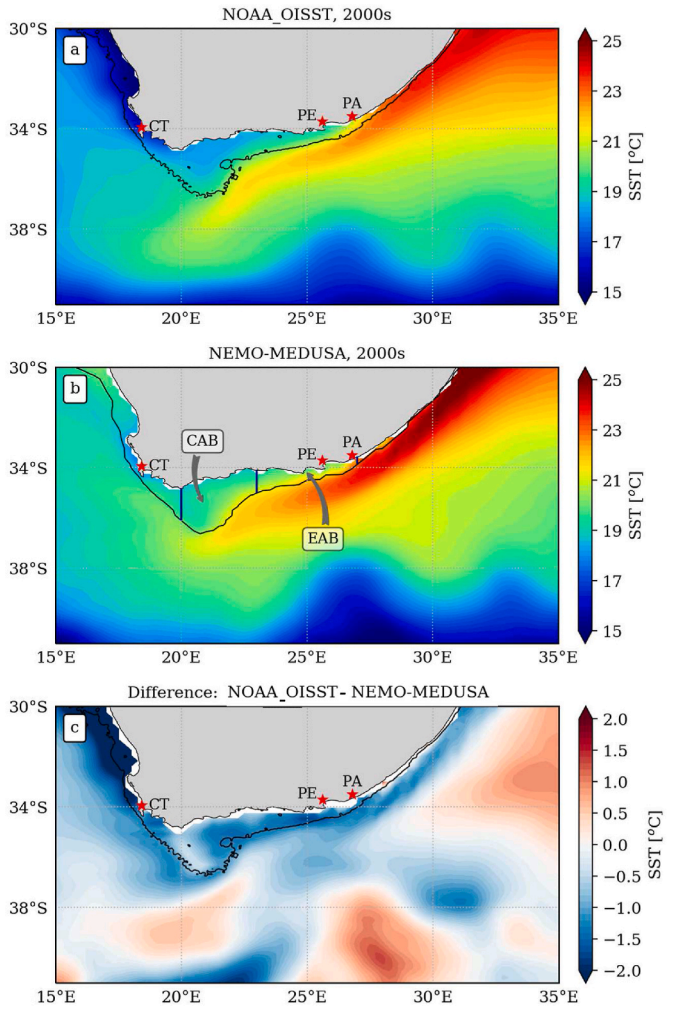

Fig. 4. (a) Observed and (b) NEMO-MEDUSA SST (°C) shown as a decadal mean, for 2000–2009. The bottom panel (c) is the difference between modelled SST (b) and observed SST (a). Observed SST are from the NOAA Optimum Interpolation. The 200 m isobath from ETOPO2 (a) and from the model (b) is overlaid as a black line. On panel (b), two different zones of the Agulhas Bank are delimited: the CAB(between 20°E and 23°E) and the EAB (between 23°E and 27°E). Boxes are used in the following figures. CT, PE and PA stand for Cape Town, Port Elizabeth and Port Alfred respectively.

absence of riverine nutrient input and the coarse resolution of the model, the productivity on the Agulhas Bank may be underestimated due to being unable to resolve coastal and shelf processes adequately.

As we are reliant on in-situ measurements of DIN, all available observations across the Agulhas Bank are shown with the modelled DIN seasonal cycle (Fig. 5c and d). The in-situ data are extremely variable with observations clustered in certain months: April, May, September, October for the CAB and May and September for the EAB. This could indicate a considerable interannual variability in addition to the heterogeneous spatial distribution (illustrated on Supplementary Fig. 3). In the model, the maximum DIN concentration occurs in austral winter (July–August) across the Agulhas Bank, with a minimum of around 0.3 mmolN.m^{-3} in austral summer-spring (from December to April). The scarcity and unbalanced distribution of in-situ data makes it difficult to effectively validate the details of the modelled DIN in this region; however, the modelled values are within the observed range.

The MLD in the model and from de Boyer Montegut's climatology (de Boyer Montégut et al., 2004) exhibit a similar seasonal cycle on the CAB, especially during the austral winter with a deeper mixed layer of 48–50 m (Fig. 5e). In summer, the mixed layer becomes more shallow with a modelled mixed layer closer to the surface (around 15 m) than in the observations (25 m). On the EAB (Fig. 5f), the MLD is shallower than on the CAB but it exhibits a similar seasonal cycle with its deepest mixed layer in winter and its shallowest in summer. The model tends to produce a shallower mixed layer compared with de Boyer Montégut's climatology on the EAB.

Whilst higher spatial resolution is required to resolve small-scale dynamics on the Agulhas Bank, NEMO-MEDUSA (1/4°) is able to simulate key aspects of ocean dynamics and biogeochemistry on the Bank.

3.2. *Future projections*

Annual means of SST, bottom temperature, integrated PP, surface DIN and MLD from 2000 to 2099 are illustrated in Fig. 6. Our analysis is based on Popova et al. (2016) and Jacobs et al. (2021) who analysed future trends of climatic stressors by looking at if those climatic stressors fall outside of the range of their "baseline variability". This baseline is a fixed period and is defined as the decadal average value over this period plus or minus two standard deviations from the mean which represent the range of variability. Here, we consider the period 2000–2009 as the baseline. A considerable increase in SST, of about 0.27 °C per decade, is evident on both parts of the Agulhas Bank, with values outside of the range of natural variability almost immediately (Fig. 6a). However, regarding gobal projections, this increase is slower compared with most of the ocean regions, especially the Northern Indian Ocean (Fig. 1c in Popova et al., 2016).

Bottom temperature (Fig. 6b) also experiences an increase, faster on the CAB but less substantial than the surface temperatures (0.17 °C/decade on the CAB and 0.10 °C/decade on the EAB), which implies an increase in stratification. Bottom temperature is projected to be outside the range of natural variability from 2030, later than SST.

Besides considerable interannual variability, especially on the CAB, projected changes in the MLD also indicate a slow shoaling of 0.4 m and 0.2 m per decade on the CAB and EAB respectively (Fig. 6c). After 2070, the MLD is consistently outside of the range of "baseline variability", projecting shallower values (above 15 m). These findings are in line with current literature that commonly associates ocean surface warming with a more stratified ocean (Capotondi et al., 2012; Li et al., 2020; Yamaguchi and Suga, 2019).

The constant shoaling of the mixed layer after 2070 is accompanied by a decrease in DIN concentration over the Agulhas Bank (Fig. 6d). However, although DIN concentrations fall below the baseline from 2060, this decrease is not enough to produce any significant response in PP (Fig. 6e). An initial increase in PP is projected until 2020 before declining until the end of the century but it remains inside the range of the baseline variability. Even though a constant MLD shoaling and a decrease in surface nitrate concentration is observed in the model, the decrease in PP that we might expect is not found. It is, however, important to note the differences with Fig. 2 which shows a significant negative trend of PP over the wider Southwest Indian Ocean domain (38°S-25°S, 19°E−45°E). This highlights that while the Southwest Indian Ocean might experience a negative trend of PP, as seen in Fig. 2, this is not necessarily representative of what really happens on the Agulhas Bank which seems to respond differently to long-term changes. Nonetheless, the lack of significant decrease in PP could be the fact that phytoplankton growth rate and, consequently, primary production increase with temperature (Yool et al., 2013a, 2013b). By the end of the century, DIN concentrations are still above 0.3 mmolN.m^{-3}, which indicates that the region is still not nutrient-limited and provides enough DIN to enable the PP. Thus, these two opposing factors (increase of temperature and decrease of DIN) cancel each other out.

The change in the spatial distribution of PP is also examined at the beginning and the end of the century (Fig. 7a and b). Fig. 7b reveals weak anomalies over the Agulhas Bank: positive anomalies of about 0.01 gC.m^{-2}.d^{-1} on the CAB (around 21°E−36°S) and negative anomalies of

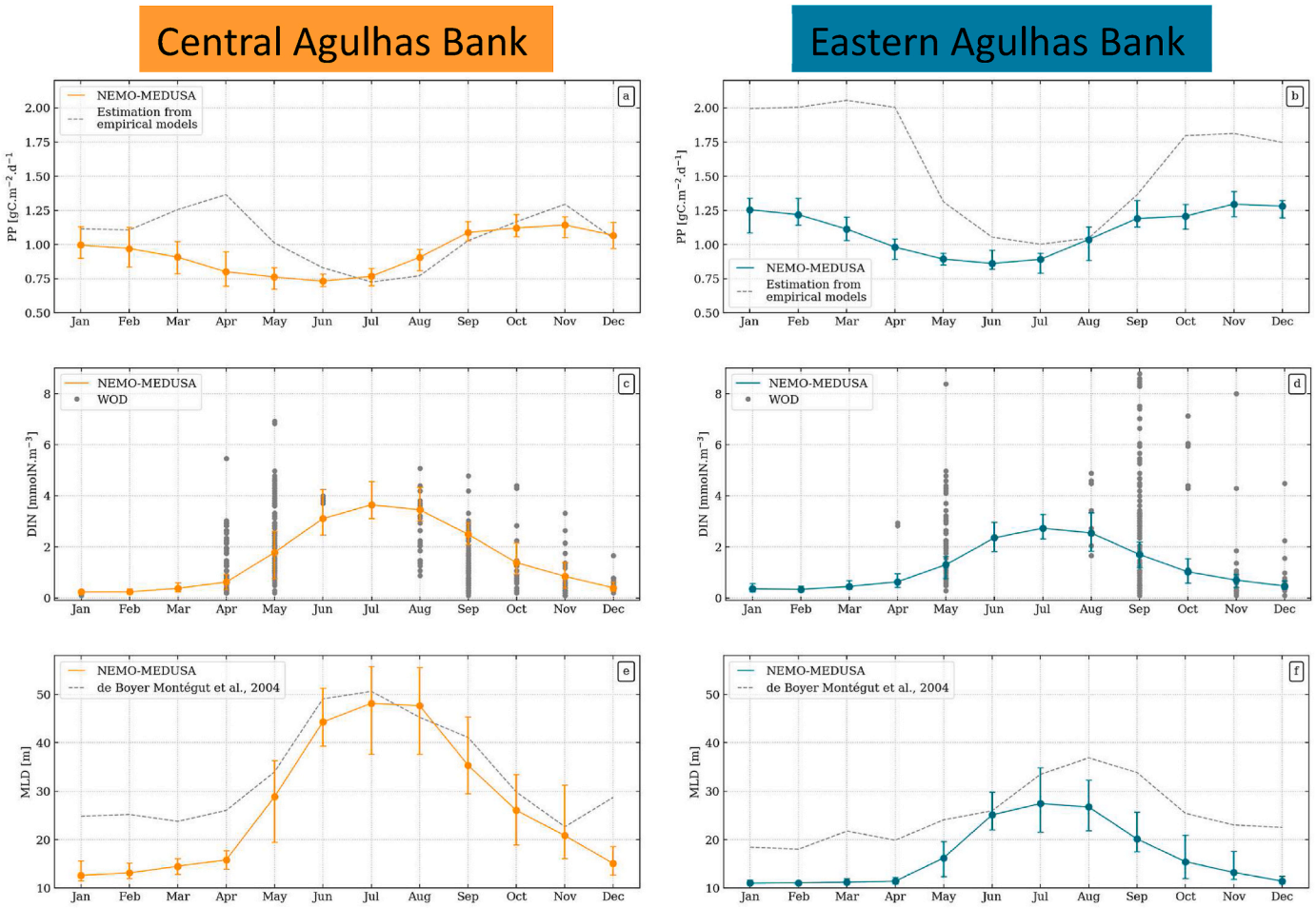

Fig. 5. Observational or estimated seasonal cycles (dashed lines and dots) and NEMO-MEDUSA seasonal cycles (solid lines) of (a,b) primary production (gC.m^{-2}.d^{-1}), (c,d) dissolved inorganic nitrogen (mmolN.m^{-3}) and (e,f) mixed layer depth (m) for 2000–2009. The modelled PP seasonal cycle is compared to an average of PP seasonal cycle estimated from three empirical models (VGPM, Eppley-VGPM and CbPM) and computed for the period 2000–2009. DIN observations are from the World Ocean Database (WOD). Rather than computing the seasonal cycle of in-situ nitrate, all observations (1963–2019) are shown because of their scarcity. The "observational" seasonal cycle of MLD comes from the global annual climatology distributed by IFREMER/LOS using temperature profiles from 1990 to 2008. Left and right panels display seasonal cycles on the Central Agulhas Bank and the Eastern Agulhas Bank respectively (see delimited areas on Fig. 2b). The vertical lines show the range of values in the model for each month.

0.04 gC.m^{-2}.d^{-1} on the EAB. Interestingly, the Agulhas Current reveals a different situation, showing a decline in productivity of ~20% from 26°E–35°S by the end of the century. Regarding the concentration of DIN, Fig. 7c and d project a general decrease across the entire domain. By the end of the 21st century, surface DIN concentrations are projected to reduce by about 33% on the Agulhas Bank: by 0.6 mmolN.m^{-3} and by 0.4 mmolN.m^{-3} over the CAB and EAB respectively. This decrease in DIN could partially be explained by a shoaling of the mixed layer over the Agulhas Bank, highlighted in Fig. 7e and f. Indeed, reduced mixing prevents the nutrients from being entrained from the deeper layers and reaching the surface but this is unlikely the only factor impacting DIN concentrations. It has been documented that wind-driven upwelling occurring along the coast and a shelf-break upwelling induced by the strong Agulhas Current bring nutrients to the surface (Goschen et al., 2015; Jackson et al., 2012; Lutjeharms et al., 1996, 2000; Malan et al., 2018).

On the southernmost point of the CAB, by the 2090s, the mixed layer has shoaled by up to 5 m and by about 1–2 m on the EAB. However, in the core of the Agulhas Current, the mixed layer deepens by about 1 m. Clearly, such an insignificant shoaling in the Agulhas Current cannot explain the projected decline of nutrients, and the explanation probably lies with non-local advective impacts. However, a full investigation of the mechanism of nutrient decline in Agulhas Current is outside of the scope of this study.

To assess changes in circulation, surface current velocities are analysed for the 2000s and 2090s (Fig. 8a and b). The difference between these two decades is also computed (Fig. 8c). The most notable change is an onshore (north-westward) shift of the Agulhas Current, indicated by the positive anomalies on the inshore side of the Agulhas Current and negative anomalies on the offshore side of the Agulhas Current. This is further demonstrated by the grey and pink dashed lines, which represent the 0.5 m s^{-1} contour for the 2000s and 2090s respectively. Fig. 8c clearly exhibits a shift of the 0.5 m s^{-1} contour onto the Agulhas Bank by the 2090s, which occurs along most of its path but is most apparent from 22 to 24°E. This could increase the likelihood of Agulhas Current water on the Agulhas Bank, affecting the temperature and surface currents, which may have implications for various species. Considerable changes are also projected in the Agulhas Return Current (southeast of 36°S, 24°E) but this is outside the scope of this study.

4. Discussion and conclusions

The waters of the Agulhas Bank are projected to undergo many changes over the course of the 21st century. In order to analyse these changes on the Agulhas Bank, future projections from the coupled model NEMO-MEDUSA are used in this study. While the model is able to

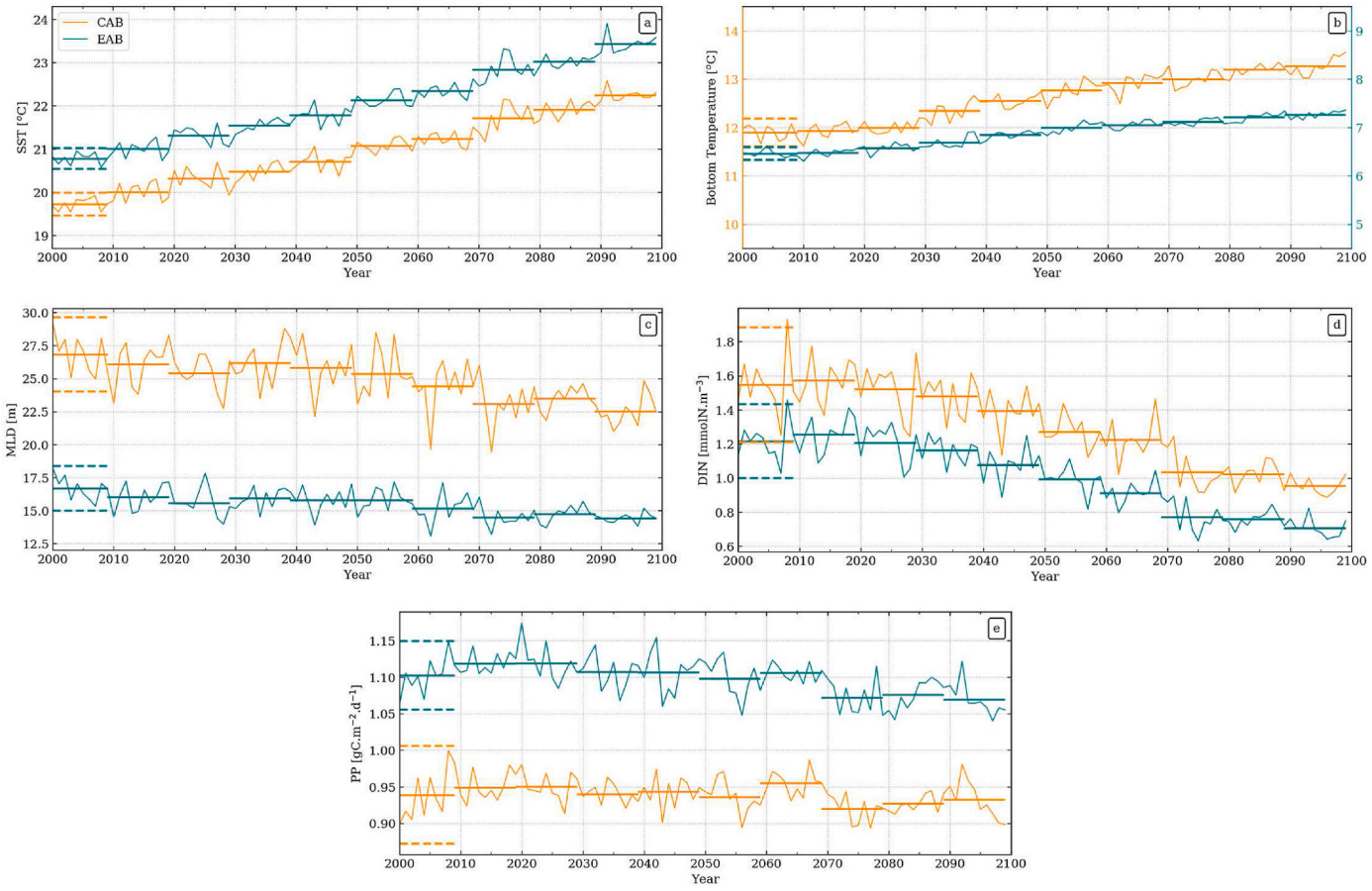

Fig. 6. Annual means of (a) SST (°C), (b) bottom temperature (°C), (c) MLD (m), (d) surface DIN(mmolN.m^{-3}) and (e) PP (gC.m^{-2}.d^{-1}) for the period 2000–2009 in NEMO-MEDUSA. Orange lines and green lines are the annual means averaged on the Central Agulhas Bank (CAB) and the Eastern Agulhas Bank (EAB) respectively (areas shown on Fig. 2b). Decadal-averaged values are shown as horizontal lines. Horizontal dashed lines are the range of variability computed for the period 2000–2009 (±2 standard deviations). Note on panel b, y-axes are different for CAB (left) and EAB (right) in order to better highlight the evolution on both parts of the Bank. A range of 5 °C is set in both cases.

represent the main dynamics and biogeochemistry reasonably well, including the Agulhas Current, the spatial resolution (1/4°) is unable to resolve some small-scale dynamics on the Bank e.g. the Cold Ridge and coastal upwelling. Additionally, since we cannot compute uncertainty estimates as the output is from a single model, care must be taken when putting these projections into the context of marine ecosystem management. As the spatial resolution of these Earth Systems Models increases, smaller-scale processes are more likely to be resolved, which will provide better understanding of future changes in this region. Despite these potential drawbacks, the model does a reasonably good job at simulating the location and strength of the Agulhas Current whilst also capturing some mesoscale variability on monthly timescales. Thus, we deem it a good choice for our study.

Popova et al. (2016) looked at future projections of some climatic stressors over multiple hotspot regions, including a wide region around South Africa (50°S-20°S, 10°E–40°E) using NEMO-MEDUSA. The authors found an increase of about 3 °C through the century, which is lower than projections for other hotspots (e.g. 4–5 °C for the Indian, east Australian and Mozambique Channel hotspots). Here, we show that projections for the Agulhas Bank are even smaller at 2 °C, which could indicate that it may be a refuge for marine species. The PP for the wider South African region is also projected to undergo a greater decline than the Agulhas Bank by 2100, giving further evidence that it could be a potential refuge. The projected SST increase of about 2 °C contrasts with bottom temperature projections of an increase by about 1.5 °C on the CAB and by 1 °C on the EAB. This surface warming, combined with a shoaling in MLD, leads to intensified stratification on the Agulhas Bank, while a deepening of the mixed layer is observed in the core of the Agulhas Current. In addition to the shallower MLD on the Bank, the model projects a reduction of surface DIN concentrations all across the Agulhas Bank and in the Agulhas Current. Despite this reduction in DIN, the model does not predict any significant change in PP on the Agulhas Bank. Poulton et al. (in this issue) shows that the phytoplankton in the upper layer of the Agulhas Bank is nitrate-limited but suggests this limitation is most likely due to the limited amount of nutrients that can penetrate the euphotic layer as nutrients are available in the bottom layer. The limited PP changes can be explained by an increase in subsurface fraction of the primary production driven by the deeper, rather than the surface nutrient concentration, and/or increase in the phytoplankton growth rate driven by the temperature increase.

These predicted oceanographic changes are likely to play an important role in recruitment of chokka squid. Roberts & van den Berg (2002) suggest that food availability on the Bank is unlikely to be a critical parameter for squid paralarvae survival, as copepods, one of the possible preys for squid paralarvae, are widely distributed across the Agulhas Bank. However, recent research has found evidence that the chokka squid catch is positively correlated to surface chlorophyll concentrations, a proxy for phytoplankton abundance (Jebri et al., in this issue). The results of this study do not show a major reduction in PP and therefore one could speculate that food is unlikely to become more limiting in the future than it is at the present day.

Warmer temperatures are likely to impact the chokka squid spawning on the Agulhas Bank. Hatching of squid eggs is temperature-dependant, with development abnormalities observed in the

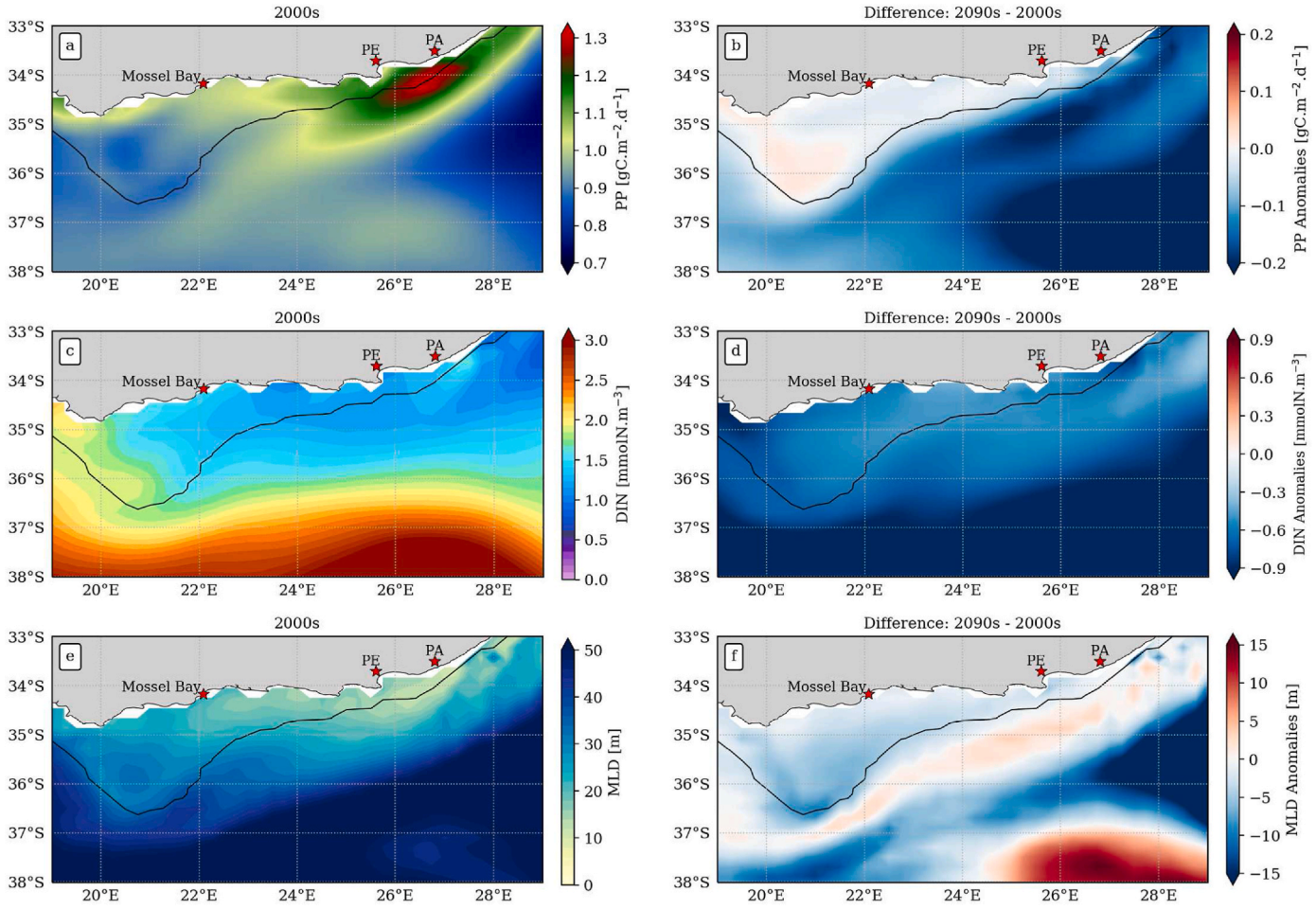

Fig. 7. (left) Decadal average for the 2000s and (right) decadal-averaged anomalies between the 2090s and the 2000s for (top panels) PP (gC.m^{-2}.d^{-1}), (middle panels) surface DIN (mmolN.m^{-3}) and (bottom panels) MLD (m) in NEMO-MEDUSA. The black line represents the 200 m isobath. PE and PA stand for Port Elizabeth and Port Alfred respectively.

laboratory at temperatures less than 12 °C and greater than 15 °C, and at water temperatures less than 9 °C and greater than 21 °C when abnormalities greatly increased (Oosthuizen et al., 2002). The developmental time of eggs will also be faster at a higher temperature. A shorter time span of egg and paralarvae stages, meaning that the adult stage is reached sooner, may have a positive impact on squid recruitment as the greater loss by advection or predation is during the early developmental stage. Despite this, the increased temperatures projected in this model predict a substantial decline in the chokka squid catch over the coming decades (see Gornall et al., in this issue). Additionally, the spawning areas on the CAB and EAB might decrease inshore spatially, causing a negative economic impact. Spawning further offshore might also lead to increased losses of paralarvae due to offshore advection. Hence, any increase in bottom water temperature is likely to impact spawning success in ways that are not yet understood and require further research.

One of the key stressors for marine ecosystems is changes to the ocean circulation (e.g. Popova et al., 2016). Rather than major changes in the speed of the Agulhas Current, here we find evidence of a projected onshore (north-westward) shift of the Agulhas Current, inducing faster flow on the Agulhas Bank. This could lead to a number of secondary changes on the Agulhas Bank. The Agulhas Current initiates shelf-edge upwelling onto the Agulhas Bank (Swart and Largier, 1987), with a faster current leading to enhanced flow of cold, nutrient-rich water onto the shelf (e.g. Russo et al., 2019), priming it for wind-driven upwelling (e.g. Leber et al., 2017). An Agulhas Current that is in closer proximity to the Bank may also enhance this shelf-edge upwelling. Current shifts have previously been found to cause changes in the distribution of species (e.g. Coleman et al., 2013; Cetina-Heredia et al., 2015). A shift of the Agulhas Current onto the Bank could be detrimental for chokka squid and many other pelagic species that spawn on the EAB and CAB. Although faster currents on the Bank enable a greater likelihood of paralarvae reaching the feeding grounds on the CAB, i.e. the Cold Ridge (e.g. Downey-Breedt et al., 2016; Jacobs et al., in this issue; Huggett et al., in this issue), there is also an enhanced risk of offshore losses (Jacobs et al., in this issue). Although there is a greater chance of the paralarvae reaching the feeding grounds, Jacobs et al. (in this issue) there is also a higher risk that they will get advected past the CAB and off the shelf before they have developed sufficiently to control their own movement. Additionally, the Agulhas Current being in closer proximity to the Bank will increase the interaction of Agulhas Bank waters with mesoscale features associated with the current, e.g. Natal Pulses, meanders and plumes, further increasing the risk of offshore losses. To understand the implications of changes in Agulhas Current position, Lagrangian experiments should be conducted in a high-resolution model (>1/12°), which is not yet available for future projections.

The combination of the increase of velocity on the Bank along with an increase in water temperature is likely to impact the distribution of various species in the long-term via impact on their growth and recruitment success. Although our approach was limited by the spatial resolution of the model which was too coarse to resolve all the key processes on the Agulhas Bank (such as wind-driven upwelling, shelf-edge upwelling or the Cold Ridge which are important features for the upward flux of nutrients), this future projection is the only one currently available for the region at resolution of 1/4°.

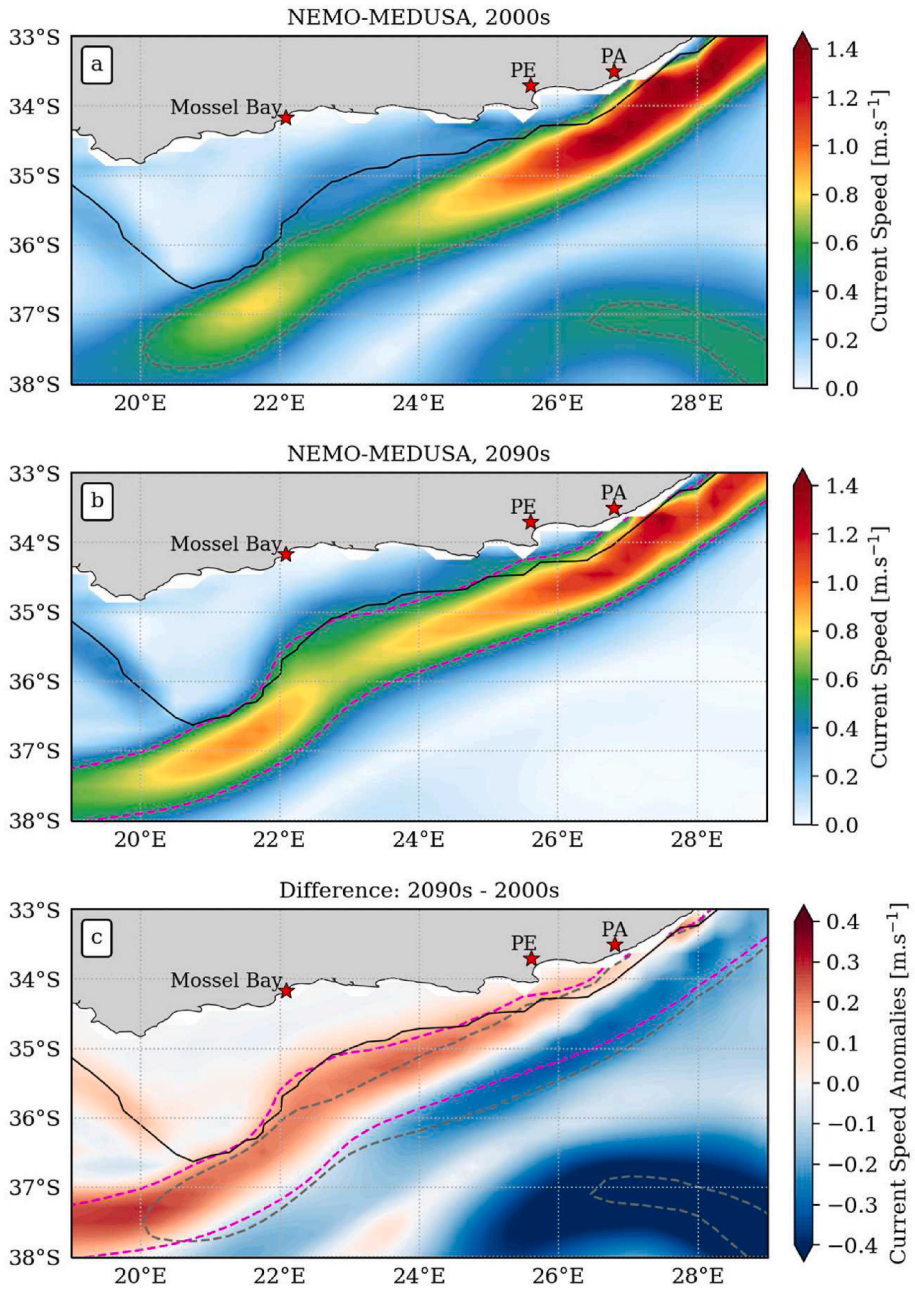

Fig. 8. Decadal-averaged surface currents (m.s^{-1}) for (a) the 2000s and (b) the 2090s. (c) Decadal-averaged anomalies between these two decades. The grey and pink dashed lines are the 0.5 m.s^{-1} contour of the Agulhas Current for the 2000s and the 2090s respectively. They represent the position of the current. The black line corresponds to the 200 m isobath. PE and PA stand for Port Elizabeth and Port Alfred respectively.

Despite the uncertainties, the NEMO-MEDUSA projections of mean PP and DIN are consistent with CMIP5 models over the wider Agulhas Current region and provide some further insights into the consequences of climate change in this region not possible from coarser resolution climate models. The projections of temperature and current patterns highlighted here will have complex biological, physiological and behavioural implications for chokka squid that are difficult to predict and may lead to serious consequences for the chokka squid fishery industry which is based in the already impoverished Eastern Cape. Improving our understanding of future changes on the Agulhas Bank by using even higher resolution models that resolve all the key processes on the Bank is critical in order to implement conservation and management plans for the region.

Author contributions

Sarah Asdar: Conceptualization, Data curation, Formal analysis, Investigation, Visualization, Writing - original draft, Writing - review and editing.

Zoe L. Jacobs: Conceptualization, Data curation, Formal analysis, Validation, Writing - original draft, Writing - review and editing.

Ekaterina Popova: Conceptualization, Project administration, Writing - review and editing.

Margaux Noyon: Formal analysis, Validation, Writing - review and editing.

Michael J. Roberts: Conceptualization, Project administration, Funding acquisition, Supervision, Writing - review and editing.

Warwick H.H. Sauer: Resources, Writing - review and editing.

Declaration of competing interest

The authors declare that they have no known competing financial interests or personal relationships that could have appeared to influence the work reported in this paper.

Acknowledgements

This publication was produced with the financial support of the Global Challenges Research Fund (GCRF) in the framework of the SOLSTICE-WIO project (NE/P021050/1). We acknowledge the NEMO consortium for the modelling framework used in this study. This work is also part of the UK-SA bilateral chair Ocean Science and Marine Food Security funded by the British Council Newton Fund grant SARCI 1503261 16102/NRF 98399. The model run was performed using the ARCHER UK National Supercomputing with outputs stored at the Centre for Environmental Data Analysis JASMIN servers.

Appendix A. Supplementary data

Supplementary data to this article can be found online at https://doi.org/10.1016/j.dsr2.2022.105092.

References

Allen, J.I., Somerfield, P.J., Gilbert, F.J., 2007. Quantifying uncertainty in high-resolution coupled hydrodynamic-ecosystem models. J. Mar. Syst. 64 (1–4), 3–14. https://doi.org/10.1016/j.jmarsys.2006.02.010.

Anav, A., Friedlingstein, P., Kidston, M., Bopp, L., Ciais, P., Cox, P., Jones, C., Jung, M., Myneni, R., Zhu, Z., 2013. Evaluating the land and ocean components of the global carbon cycle in the CMIP5 earth system models. J. Clim. 26 (18), 6801–6843. https://doi.org/10.1175/JCLI-D-12-00417.1.

Backeberg, B.C., Penven, P., Rouault, M., 2012. Impact of intensified Indian Ocean winds on mesoscale variability in the Agulhas system. Nat. Clim. Change 2 (8), 608–612. https://doi.org/10.1038/nclimate1587.

Banks, S.C., Ling, S.D., Johnson, C.R., Piggott, M.P., Williamson, J.E., Beheregaray, L.B., 2010. Genetic structure of a recent climate change-driven range extension. Mol. Ecol. 19 (10), 2011–2024. https://doi.org/10.1111/j.1365-294X.2010.04627.x.

Banzon, V., Smith, T.M., Chin, T.M., Liu, C., Hankins, W., 2016. A long-term record of blended satellite and in situ sea-surface temperature for climate monitoring, modeling and environmental studies. Earth Syst. Sci. Data 8 (1), 165–176. https://doi.org/10.5194/essd-8-165-2016.

Bao, Y., Li, Y., 2016. Simulations of dissolved oxygen concentration in CMIP5 Earth system models. Acta Oceanol. Sin. 35 (12), 28–37. https://doi.org/10.1007/s13131-016-0959-x.

Beal, L.M., Elipot, S., 2016. Broadening not strengthening of the Agulhas Current since the early 1990s. Nature 540 (7634), 570–573. https://doi.org/10.1038/nature19853.

Behrenfeld, M.J., Falkowski, P.G., 1997. Photosynthetic rates derived from satellite-based chlorophyll concentration. Limnol. Oceanogr. 42 (1), 1–20. https://doi.org/10.4319/lo.1997.42.1.0001.

Bopp, L., Resplandy, L., Orr, J.C., Doney, S.C., Dunne, J.P., Gehlen, M., Halloran, P., Heinze, C., Ilyina, T., Séférian, R., Tjiputra, J., Vichi, M., 2013. Multiple stressors of ocean ecosystems in the 21st century: projections with CMIP5 models. Biogeosciences 10 (10), 6225–6245. https://doi.org/10.5194/bg-10-6225-2013.

Boyd, A.J., Shillington, F.A., 1994. Physical forcing and circulation patterns on the Agulhas Bank. South Afr. J. Sci. 90 (3), 144. https://doi.org/10.1093/oxfordjournals.afraf.a100309, 122.

Boyer, T.P., Baranova, O.K., Coleman, C., Garcia, H.E., Grodsky, A., Locarnini, R.A., Mishonov, A.V., Paver, C.R., Reagan, J.R., Seidov, D., Smolyar, I.V., Weathers, K., Zweng, M.M., 2019. World Ocean Database 2018.

Brierley, A.S., Kingsford, M.J., 2009. Impacts of climate change on marine organisms and ecosystems. In: Current Biology, vol. 19. https://doi.org/10.1016/j.cub.2009.05.046. Issue 14.

Brown, C.J., Fulton, E.A., Hobday, A.J., Matear, R.J., Possingham, H.P., Bulman, C., Christensen, V., Forrest, R.E., Gehrke, P.C., Gribble, N.A., GRIFFITHS, S.P., Lozano-Montes, H., Martin, J.M., Metcalf, S., Okey, T.A., Watson, R., Richardson, A.J., 2010. Effects of climate-driven primary production change on marine food webs: implications for fisheries and conservation. Global Change Biol. 16 (4), 1194–1212. https://doi.org/10.1111/j.1365-2486.2009.02046.x.

Cabré, A., Marinov, I., Leung, S., 2015. Consistent global responses of marine ecosystems to future climate change across the IPCC AR5 earth system models. Clim. Dynam. 45 (5), 1253–1280. https://doi.org/10.1007/s00382-014-2374-3.

Capotondi, A., Alexander, M.A., Bond, N.A., Curchitser, E.N., Scott, J.D., 2012. Enhanced upper ocean stratification with climate change in the CMIP3 models. J. Geophys. Res.: Oceans 117 (4). https://doi.org/10.1029/2011JC007409.

Carr, M.E., Friedrichs, M.A.M., Schmeltz, M., Noguchi Aita, M., Antoine, D., Arrigo, K.R., Asanuma, I., Aumont, O., Barber, R., Behrenfeld, M., Bidigare, R., Buitenhuis, E.T., Campbell, J., Ciotti, A., Dierssen, H., Dowell, M., Dunne, J., Esaias, W., Gentili, B., Yamanaka, Y., 2006. A comparison of global estimates of marine primary production from ocean color. Deep-Sea Res. Part II Top. Stud. Oceanogr. 53 (5–7), 741–770. https://doi.org/10.1016/j.dsr2.2006.01.028.

Cetina-Heredia, P., Roughan, M., van Sebille, E., Feng, M., Coleman, M.A., 2015. Strengthened currents override the effect of warming on lobster larval dispersal and survival. Global Change Biol. 21 (12), 4377–4386. https://doi.org/10.1111/gcb.13063.

Cochrane, K.L., Joyner, J., Sauer, W., Swan, J., 2015. Final Report Informing Effective Policies for Responsible Marine Fisheries in South Africa . A Report Prepared for WWF: South Africa and the Responsible Fisheries Alliance.

Cochrane, K.L., Oliver, B., Sauer, W., 2014. An assessment of the current status of the chokka squid fishery in South Africa and an evaluation of alternative allocation strategies. Mar. Pol. 43, 149–163. https://doi.org/10.1016/j.marpol.2013.05.006.

Coleman, M.A., Feng, M., Roughan, M., Cetina-Heredia, P., Connell, S.D., 2013. Temperate shelf water dispersal by Australian boundary currents: implications for population connectivity. Limnol. Oceanogr. Fluid. Environ. 3 (1), 295–309. https://doi.org/10.1215/21573689-2409306.

Collins, W.J., Bellouin, N., Doutriaux-Boucher, M., Gedney, N., Halloran, P., Hinton, T., Hughes, J., Jones, C.D., Joshi, M., Liddicoat, S., Martin, G., O'Connor, F., Rae, J., Senior, C., Sitch, S., Totterdell, I., Wiltshire, A., Woodward, S., 2011. Development and evaluation of an earth-system model - HadGEM2. Geosci. Model Dev. (GMD) 4 (4), 1051–1075. https://doi.org/10.5194/gmd-4-1051-2011.

Cury, P., Bakun, A., Crawford, R.J.M., Jarre, A., Quiñones, R.A., Shannon, L.J., Verheye, H.M., 2000. Small pelagics in upwelling systems: patterns of interaction and structural changes in "wasp-waist" ecosystems. ICES (Int. Counc. Explor. Sea) J. Mar. Sci. 57 (3), 603–618. https://doi.org/10.1006/jmsc.2000.0712.

de Boyer Montégut, C., Madec, G., Fischer, A.S., Lazar, A., Iudicone, D., 2004. Mixed layer depth over the global ocean: an examination of profile data and a profile-based climatology. J. Geophys. Res. 109 (C12), C12003. https://doi.org/10.1029/2004JC002378.

Downey-Breedt, N.J., Roberts, M.J., Sauer, W.H.H., Chang, N., 2016. Modelling transport of inshore and deep-spawned chokka squid (Loligo reynaudi) paralarvae off South Africa: the potential contribution of deep spawning to recruitment. Fish. Oceanogr. 25 (1), 28–43. https://doi.org/10.1111/fog.12132.

Downey, N.J., Roberts, M.J., Baird, D., 2010. An investigation of the spawning behaviour of the chokka squid Loligo reynaudii and the potential effects of temperature using acoustic telemetry. ICES (Int. Counc. Explor. Sea) J. Mar. Sci. 67 (2), 231–243. https://doi.org/10.1093/icesjms/fsp237.

Frusher, S.D., Hobday, A.J., Jennings, S.M., Creighton, C., D'Silva, D., Haward, M., Holbrook, N.J., Nursey-Bray, M., Pecl, G.T., van Putten, E.I., 2014. The short history of research in a marine climate change hotspot: from anecdote to adaptation in south-east Australia. Rev. Fish Biol. Fish. 24 (2), 593–611. https://doi.org/10.1007/s11160-013-9325-7.

Garcia, H.E., Locarnini, R.A., Boyer, T.P., Antonov, J.I., Baranova, O.K., Zweng, M.M., Reagan, J.R., Johnson, D.R., Mishonov, A.V., Levitus, S., 2013. World ocean atlas 2013. In: Dissolved Inorganic Nutrients (Phosphate, Nitrate, Silicate), vol. 4. https://doi.org/10.7289/V5J67DWD.

Gornall, J. This issue. In pursuit of the holy grail of chokka squid prediction – temperature vs catch. Deep Sea Res. Part II Top. Stud. Oceanogr..

Goschen, W.S., Bornman, T.G., Deyzel, S.H.P., Schumann, E.H., 2015. Coastal upwelling on the far Eastern Agulhas Bank associated with large meanders in the Agulhas Current. Continent. Shelf Res. 101, 34–46. https://doi.org/10.1016/j.csr.2015.04.004.

Hancke, L., 2010. *Dynamics of the Tsitsikamma Current , with Implications for Larval Transport of Chokka Squid (Loligo Reyneuait) on the Eastern Agulhas Bank* (Issue February).

Hobday, A.J., Pecl, G.T., 2014. Identification of global marine hotspots: sentinels for change and vanguards for adaptation action. Rev. Fish Biol. Fish. 24 (2), 415–425. https://doi.org/10.1007/s11160-013-9326-6.

Huggett, J. This issue. Patterns in the plankton – spatial distribution and long-term variability of copepod biomass on the Agulhas Bank. Deep Sea Res. Part II Top. Stud. Oceanogr..

Hoegh-Guldberg, O., Bruno, J.F., 2010. The impact of climate change on the world's marine ecosystems. In: Science, vol. 328, pp. 1523–1528. https://doi.org/10.1126/science.1189930, 5985.

Ilyina, T., Six, K.D., Segschneider, J., Maier-Reimer, E., Li, H., Núñez-Riboni, I., 2013. Global ocean biogeochemistry model HAMOCC: model architecture and performance as component of the MPI-Earth system model in different CMIP5 experimental realizations. J. Adv. Model. Earth Syst. 5 (2), 287–315. https://doi.org/10.1029/2012MS000178.

Jackson, J.M., Rainville, L., Roberts, M.J., McQuaid, C.D., Lutjeharms, J.R.E., 2012. Mesoscale bio-physical interactions between the Agulhas current and the Agulhas Bank, South Africa. Continent. Shelf Res. 49, 10–24. https://doi.org/10.1016/j.csr.2012.09.005.

Jacobs, Z.L., Jebri, F., Raitsos, D.E., Popova, E., Srokosz, M., Painter, S.C., Nencioli, F., Roberts, M., Kamau, J., Palmer, M., Wihsgott, J., 2020. Shelf-break upwelling and productivity over the North Kenya banks: the importance of large-scale ocean dynamics. J. Geophys. Res.: Oceans 125 (1), e2019JC015519. https://doi.org/10.1029/2019JC015519.

Jacobs, Z.L., Yool, A., Jebri, F., Srokosz, M., van Gennip, S., Kelly, S.J., Roberts, M., Sauer, W., Queirós, A.M., Osuka, K.E., Samoilys, M., Becker, A.E., Popova, E., 2021. Key climate change stressors of marine ecosystems along the path of the East African coastal current. Ocean Coast Manag. 208, 105627. https://doi.org/10.1016/j.ocecoaman.2021.105627.

Jacobs, Z.L., Roberts, M.J., Jebri, F., Srokosz, M., Kelly, S., Sauer, W.H.H., Popova, E. This issue. Drivers of productivity on the Agulhas Bank and the importance for marine ecosystems. Deep Sea Res. Part II Top. Stud. Oceanogr..

Jebri, F., Raitsos, D. E., Gittings, J. A., Jacobs, Z. L., Srokosz, M., Gornall, J., Sauer, W. H. H., Roberts, M. J., & Popova, E. This issue. Unravelling links between squid catch variations and biophysical mechanisms in South African waters. Deep Sea Res. Part II Top. Stud. Oceanogr., 196, 105028. https://doi.org/10.1016/J.DSR2.2022.105028.

Joyner, J.M., 2015. The Influence of Environmental Variability on the Catch of Chokka, Loligo Reynaudii, off the Coast of South Africa. Doctoral Dissertation. Rhodes University.

Kwiatkowski, L., Torres, O., Bopp, L., Aumont, O., Chamberlain, M., Christian, R., J., P. Dunne, J., Gehlen, M., Ilyina, T., G. John, J., Lenton, A., Li, H., Lovenduski, S., N., C. Orr, J., Palmieri, J., Santana-Falcón, Y., Schwinger, J., Séférian, R., A. Stock, C., Ziehn, T., 2020. Twenty-first century ocean warming, acidification, deoxygenation, and upper-ocean nutrient and primary production decline from CMIP6 model projections. Biogeosciences 17 (13), 3439–3470. https://doi.org/10.5194/bg-17-3439-2020.

Leber, G.M., Beal, L.M., Elipot, S., 2017. Wind and current forcing combine to drive strong upwelling in the Agulhas Current. J. Phys. Oceanogr. 47 (1), 123–134. https://doi.org/10.1175/JPO-D-16-0079.1.

Li, G., Cheng, L., Zhu, J., Trenberth, K.E., Mann, M.E., Abraham, J.P., 2020. Increasing ocean stratification over the past half-century. Nat. Clim. Change 10 (12), 1116–1123. https://doi.org/10.1038/s41558-020-00918-2.

Lutjeharms, J.R.E., Meyer, A.A., Ansorge, I.J., Eagle, G.A., Orren, M.J., 1996. The nutrient characteristics of the Agulhas bank. S. Afr. J. Mar. Sci. 17, 253–274. https://doi.org/10.2989/025776196784158464.

Lutjeharms, J.R.E., Cooper, J., Roberts, M., 2000. Upwelling at the inshore edge of the Agulhas current. Continent. Shelf Res. 20 (7), 737–761. https://doi.org/10.1016/S0278-4343(99)00092-8.

Lutjeharms, J.R.E., Monteiro, P.M.S., Tyson, P.D., Obura, D., 2001. The oceans around southern Africa and regional effects of global change. South Afr. J. Sci. 97 (3–4), 119–130.

Madec, G., 2008. NEMO reference manual, ocean dynamic component: NEMO-OPA, Note du Pôle de modélisation.

Malan, N., Backeberg, B., Biastoch, A., Durgadoo, J.v., Samuelsen, A., Reason, C., Hermes, J., 2018. Agulhas current meanders facilitate shelf-slope exchange on the Eastern Agulhas Bank. J. Geophys. Res.: Oceans 123 (7), 4762–4778. https://doi.org/10.1029/2017JC013602.

Matear, R.J., Chamberlain, M.A., Sun, C., Feng, M., 2013. Climate change projection of the Tasman Sea from an eddy-resolving ocean model. J. Geophys. Res.: Oceans 118 (6), 2961–2976. https://doi.org/10.1002/jgrc.20202.

Mathis, J.T., Cooley, S.R., Lucey, N., Colt, S., Ekstrom, J., Hurst, T., Hauri, C., Evans, W., Cross, J.N., Feely, R.A., 2015. Ocean acidification risk assessment for Alaska's fishery sector. Prog. Oceanogr. 136, 71–91. https://doi.org/10.1016/j.pocean.2014.07.001.

Mohan, S., Bhaskaran, P.K., 2020. Evaluation and bias correction of global climate models in the CMIP5 over the Indian Ocean region. Environ. Monit. Assess. 191 (3), 806. https://doi.org/10.1007/s10661-019-7700-0.

Ntola, B.P., 2010. In: Analysis of the Chokka Squid. Loligo reynaudi d`Orbigny, p. 1845. *; log-book data in South Africa.* Universitetet i Tromsø. https://munin.uit.no/handle/10037/2483.

Okey, T.A., Alidina, H.M., Lo, V., Jessen, S., 2014. Effects of climate change on Canada's Pacific marine ecosystems: a summary of scientific knowledge. Rev. Fish Biol. Fish. 24 (2), 519–559. https://doi.org/10.1007/s11160-014-9342-1.

Oosthuizen, A., Roberts, M.J., Sauer, W.H.H., 2002. Temperature effects on the embryonic development and hatching success of the squid Loligo vulgaris reynaudii. Bull. Mar. Sci. 71. Issue 2.

Pecl, G.T., Hobday, A.J., Frusher, S., Sauer, W.H.H., Bates, A.E., 2014. Ocean warming hotspots provide early warning laboratories for climate change impacts. May 4 Rev. Fish Biol. Fish. 24 (2), 409–413. https://doi.org/10.1007/s11160-014-9355-9.

Poloczanska, E.S., Babcock, R.C., Butler, A., Hobday, A.J., Hoegh-Guldberg, O., Kunz, T. J., Matear, R., Milton, D.A., Okey, T.A., Richardson, A.J., 2007. Climate change and Australian marine life. In: Oceanography and Marine Biology, vol. 45. https://doi.org/10.1201/9781420050943.ch8. Issue June).

Poloczanska, E.S., Burrows, M.T., Brown, C.J., Molinos, J.G., Halpern, B.S., Hoegh-Guldberg, O., Kappel, C.V., Moore, P.J., Richardson, A.J., Schoeman, D.S., Sydeman, W.J., 2016. Responses of marine organisms to climate change across oceans. In: Frontiers in Marine Science, vol. 3. Frontiers Media S. A, p. 62. https://doi.org/10.3389/fmars.2016.00062. Issue MAY.

Poulton, A.J., Mazwane, S.L., Godfrey, B., Carvalho, A., Mawji, E., Wihsgott, J.U., Noyon, M., March 2019. This issue. Primary production dynamics on the Agulhas Bank in autumn. Deep Sea Res. Part II Top. Stud. Oceanogr.

Popova, E.E., Yool, A., Coward, A.C., Aksenov, Y.K., Alderson, S.G., de Cuevas, B.A., Anderson, T.R., 2010. Control of primary production in the Arctic by nutrients and light: insights from a high resolution ocean general circulation model. Biogeosci. Discuss. 7 (4), 5557–5620. https://doi.org/10.5194/bgd-7-5557-2010.

Popova, E.E., Yool, A., Byfield, V., Cochrane, K., Coward, A.C., Salim, S.S., Gasalla, M.A., Henson, S.A., Hobday, A.J., Pecl, G.T., Sauer, W.H., Roberts, M.J., 2016. From global to regional and back again: common climate stressors of marine ecosystems relevant for adaptation across five ocean warming hotspots. Global Change Biol. 22 (6), 2038–2053. https://doi.org/10.1111/gcb.13247.

Potts, W.M., Götz, A., James, N., 2015. Review of the projected impacts of climate change on coastal fishes in southern Africa. In: Reviews in Fish Biology and Fisheries, vol. 25. Springer International Publishing, pp. 603–630. https://doi.org/10.1007/s11160-015-9399-5, 4.

Riahi, K., Rao, S., Krey, V., Cho, C., Chirkov, V., Fischer, G., Kindermann, G., Nakicenovic, N., Rafaj, P., 2011. RCP 8.5-A scenario of comparatively high greenhouse gas emissions. Climatic Change 109 (1), 33–57. https://doi.org/10.1007/s10584-011-0149-y.

Rickard, G., Behrens, E., 2016. CMIP5 earth system models with biogeochemistry: a Ross Sea assessment. Antarct. Sci. 28 (5), 327–346. https://doi.org/10.1017/S0954102016000122.

Rio, M.-H., Mulet, S., Picot, N., 2014. Beyond GOCE for the ocean circulation estimate: synergetic use of altimetry, gravimetry, and in situ data provides new insight into geostrophic and Ekman currents. Geophys. Res. Lett. 41 (24), 8918–8925. https://doi.org/10.1002/2014GL061773.

Roberts, M.J., van den Berg, M., 2002. Recruitment variability of chokka squid (Loligo vulgaris reynaudii): role of currents on the Agulhas Bank (South Africa) in paralarvae distribution and food abundance. Bull. Mar. Sci. 71 (2), 691–710.

Roberts, M.J., 2005. Chokka squid (Loligo vulgaris reynaudii) abundance linked to changes in South Africa's Agulhas Bank ecosystem during spawning and the early life cycle. ICES (Int. Counc. Explor. Sea) J. Mar. Sci. 62 (1), 33–55. https://doi.org/10.1016/j.icesjms.2004.10.002.

Roberts, M. J.,This issue. The South African squid fishery – why do catches crash intermittently? Deep Sea Res. Part II Top. Stud. Oceanogr..

Robinson, J., Popova, E.E., Srokosz, M.A., Yool, A., 2016. A tale of three islands: downstream natural iron fertilization in the Southern Ocean. J. Geophys. Res.: Oceans 121 (5), 3350–3371. https://doi.org/10.1002/2015JC011319.

Rouault, M., Penven, P., Pohl, B., 2009. Warming in the Agulhas current system since the 1980's. Geophys. Res. Lett. 36 (12), 2–6. https://doi.org/10.1029/2009GL037987.

Roy, C., Van Der Lingen, C.D., Coetzee, J.C., Lutjeharms, J.R.E., 2007. Abrupt environmental shift associated with changes in the distribution of Cape anchovy Engraulis encrasicolus spawners in the southern Benguela. Afr. J. Mar. Sci. 29 (3), 309–319. https://doi.org/10.2989/AJMS.2007.29.3.1.331.

Russo, C.S., Lamont, T., Tutt, G.C.O., van den Berg, M.A., Barlow, R.G., 2019. Hydrography of a shelf ecosystem inshore of a major Western Boundary Current. Estuar. Coast Shelf Sci. 228, 106363. https://doi.org/10.1016/j.ecss.2019.106363.

Séférian, R., Bopp, L., Gehlen, M., Orr, J.C., Ethé, C., Cadule, P., Aumont, O., Salas y Mélia, D., Voldoire, A., Madec, G., 2013. Skill assessment of three earth system models with common marine biogeochemistry. Clim. Dynam. 40 (9), 2549–2573. https://doi.org/10.1007/s00382-012-1362-8.

Srokosz, M.A., Robinson, J., McGrain, H., Popova, E.E., Yool, A., 2015. Could the Madagascar bloom be fertilized by Madagascan iron? J. Geophys. Res.: Oceans 120 (8), 5790–5803. https://doi.org/10.1002/2015JC011075.

Stow, C.A., Jolliff, J., McGillicuddy, D.J., Doney, S.C., Allen, J.I., Friedrichs, M.A.M., Rose, K.A., Wallhead, P., 2009. Skill assessment for coupled biological/physical models of marine systems. J. Mar. Syst. 76 (1), 4–15. https://doi.org/10.1016/j.jmarsys.2008.03.011.

Swart, V.P., Largier, J.L., 1987. Thermal structure of Agulhas Bank water. S. Afr. J. Mar. Sci. 5 (1), 243–252. https://doi.org/10.2989/025776187784522153.

Taylor, K.E., Stouffer, R.J., Meehl, G.A., 2012. An overview of CMIP5 and the experiment design. Bull. Am. Meteorol. Soc. 93 (4), 485–498. https://doi.org/10.1175/BAMS-D-11-00094.1.

Timmermann, R., Goosse, H., Madec, G., Fichefet, T., Ethe, C., Dulière, V., 2005. On the representation of high latitude processes in the ORCA-LIM global coupled sea ice-ocean model. Ocean Model. 8 (1–2), 175–201. https://doi.org/10.1016/j.ocemod.2003.12.009.

van Gennip, S.J., Popova, E.E., Yool, A., Pecl, G.T., Hobday, A.J., Sorte, C.J.B., 2017. Going with the flow: the role of ocean circulation in global marine ecosystems under a changing climate. Global Change Biol. 23 (7), 2602–2617. https://doi.org/10.1111/gcb.13586.

Wassmann, P., Duarte, C.M., Agustí, S., Sejr, M.K., 2011. Footprints of climate change in the Arctic marine ecosystem. Global Change Biol. 17 (2), 1235–1249. https://doi.org/10.1111/j.1365-2486.2010.02311.x.

Westberry, T., Behrenfeld, M.J., Siegel, D.A., Boss, E., 2008. Carbon-based primary productivity modeling with vertically resolved photoacclimation. Global Biogeochem. Cycles 22 (2). https://doi.org/10.1029/2007GB003078 n/a-n/a.

Wu, L., Cai, W., Zhang, L., Nakamura, H., Timmermann, A., Joyce, T., McPhaden, M.J., Alexander, M., Qiu, B., Visbeck, M., Chang, P., Giese, B., 2012. Enhanced warming over the global subtropical western boundary currents. Nat. Clim. Change 2 (3), 161–166. https://doi.org/10.1038/nclimate1353.

Yamaguchi, R., Suga, T., 2019. Trend and variability in global upper-ocean stratification since the 1960s. J. Geophys. Res.: Oceans 124 (12), 8933–8948. https://doi.org/10.1029/2019JC015439.

Yool, A., Popova, E.E., Anderson, T.R., 2013a. MEDUSA-2.0: an intermediate complexity biogeochemical model of the marine carbon cycle for climate change and ocean acidification studies. Geosci. Model Dev. (GMD) 6 (5), 1767–1811. https://doi.org/10.5194/gmd-6-1767-2013.

Yool, A., Popova, E.E., Coward, A.C., 2015. Future change in ocean productivity : is the Arctic the new Atlantic? Geophys. Res. 120, 7771–7790. https://doi.org/10.1002/2015JC011167.

Yool, A., Popova, E.E., Coward, A.C., Bernie, D., Anderson, T.R., 2013b. Climate change and ocean acidification impacts on lower trophic levels and the export of organic carbon to the deep ocean. Biogeosciences 10 (9), 5831–5854. https://doi.org/10.5194/bg-10-5831-2013.